Structural Behaviour of RC Beam-To-Column Connection with Corroded Shear Reinforcement

Charles K. S. Moy
Department of Civil Engineering, Xi'an Jiaotong-Liverpool University, Suzhou, Jiangsu, China
Email: charles-loo@hotmail.com

***Abstract*—Corrosion of steel reinforcement in reinforced concrete structures is a serious factor affecting their lifespan. There are more and more studies devoted to understanding the influence of corrosion on RC structures. Recent studies have focused on shear strength deterioration of RC beams since shear failure are often sudden leading to disastrous consequences. However, there is still a lack of understanding when it comes to beam-to-column connections, particularly connections with shear critical beams. This study provides much needed information about the structural behaviour of shear critical beam-to-column connections with corroded shear links. Full scale samples were tested for that purpose. The deterioration was monitored under constant static loading. It was found that the targeted 20% corroded shear link resulted in 13.5 – 17% loss in ultimate strength. The rotational stiffnesses were also greatly affected. The crack pattern helped to interpret the load path and the subsequent deterioration of the structure.**

***Index Terms*—corrosion, shear reinforcement, RC beam to column connection, failure mode**

I. Introduction

Reinforced Concrete (RC) is widely used to construct structures such as buildings and bridges. The combination of steel and concrete is considered highly efficient and durable. However, one of the major hindrances that can affect reinforced concrete is corrosion of the steel reinforcement. Corrosion in RC structures usually occur due to the exposure of the steel to the environment as a result of damage of the concrete cover. The subsequent deterioration is the result of three factors; (i) the corrosion product, rust will reside at the interface between reinforcement and concrete, which induce interior pressure, (ii) losses in the effective cross-section area of concrete due to cracking and (iii) losses in the mechanical performance of the reinforced bars due to losses in their cross-sectional area [1]. Furthermore, the maximum bond strength and the bond rigidity will decrease proportionally to the increase of corrosion percentage [2] and its induced pressure, which increases due to expansion of the rebar. Hence, the lifespan of reinforced concrete depends heavily on the environment surrounding it. For example, coastal or marine RC structures are more prone to corrosion as the chloride favours corrosion. Numerous studies are devoted to studying the influence of corrosion on reinforced concrete beams. Most of them focus on flexural and bond strength loss (see for e.g. [3]-[5]) and only a few studies are related to the shear strength deterioration of beams [6]-[9]. The corrosion effect on the shear strength capacity is of particular interest since it is likely to result in sudden failure. This is aggravated by the fact that shear links are more susceptible to corrosion, having less cover protection than the main bars.

To date, studies were mostly focused on the corrosion effect on reinforced concrete beams. For example, Rodriguez *et al*. (1997) investigated the failure behaviour of concrete beam specimens corroded at a constant rate of 0.1 mA/cm^2 in calcium chloride solution [10]. In addition to a deterioration of the shear strength, the effect of pitting corrosion and concrete cover cracking and spalling were severe. Xia *et al.* (2011) found that there was a correlation between the crack widths and the mass loss of the shear reinforcement [11]. They also noticed that the shear failure mode changed from concrete crushing to stirrup failure for increasing corrosion levels. Another similar study was performed by Zhu *et al.* (2013) but conducted the study on specimens exposed to a chloride environment for 26 years [12]. All the beams failed suddenly with brittle shear fracture. Similar observations were recorded by Lachemi *et al*. (2014) [13].

The ultimate shear strength is dependent on the amount of the shear reinforcement which in turn affects the shear failure mode. Shear failure can occur in two forms; shear tension failure or shear compression failure. Under applied shear force, split cracks along the main bar will develop and subsequent bond deterioration will occur in a wide region [14]. Hence, the inclusion of stirrups usually results in higher shear strength, controlled deformation and less crack formation. Shear failure is known to occur with little warning [15]. Generally, the size of the beam will affect the shear capacity in longitudinally reinforced concrete members. Slowik (2014) showed that both the slenderness ratio or effective length-to-depth and the shear span ratio will affect the failure mechanism [16].

Beam to column connection is critical in a structure. The geometry and force distribution at the joint region is crucial to predict the failure of a frame [17]. A moment resisting connection usually requires an adequate anchorage length of the main bars from the beam into the column. Studies to understand beam-to-column connection requires the moment-rotation curves to assess

Manuscript received July 20, 2016; revised November 28, 2016.

doi: 10.18178/ijscer.6.2.83-88

the joint stiffness. Alva and El Debs (2013) observed slippage of such connection in the disturbed region [18]. They proposed two mechanisms to explain the failure at the joint. The first mechanism is a slip between the beam and the column resulting in a small rotation. The second mechanism is a rotation of the beam due to localized slops caused by cracking for a certain length at the top bar. To the author's knowledge there is no known study that investigates the effect of corrosion on shear load transfer of a beam to column connection. This study brings in valuable information to understand the failure mechanism of corroded shear link for a beam to column connection.

II. Methodology

A. Test Specimens

A total of 8 beam to column specimens were casted. Two of the beams were used as control and six beams were corroded. The main bars were high-strength steel having yield strengths of around 450 MPa and the shear links were mild steel having a yield strength of 250 MPa. The concrete were Grade 30 ready mix concrete obtained from the local ready mix concrete plant. The beam and the column were designed according to Australian Standard AS 3600-2009 [19]. The details of the test specimens are shown in Fig. 1. The beam size was 200 mm x 300 mm x 1000 mm while the column was 230 mm x 230 mm x 2000 mm. The beams were designed to be shear critical with two layers of 2Y25 top bars placed in the tension region and 3Y16 bottom bars placed in the compression region. R6 closed shear links were placed at 300 mm centre to centre. The columns were reinforced with 4Y16 bars with R8 ties spaced at 200 mm centres.

B. Concrete Compressive Strength

The concrete compressive strength was tested for 7, 14 and 28 days in accordance with British Standards (BS EN 12390-32009). The recorded compressive strength was averaged from 3 cubes for each batch of concrete.

C. Accelerated Corrosion

The accelerated corrosion was performed using 4% chloride solution in a purpose-built basin. A DC power supply with a limit of 3 V and a maximum of 3 A was used to apply a constant current of 0.25 mA/cm^2 to the specimens. The shear link was connected to the positive terminal as the anode and a piece of stainless steel bar was used as the cathode. All the other reinforcement bars were protected using K'mastic 5000 epoxy paint that provides high chemical and moisture protection to ensure that only the selected shear link is corroded. The targeted corrosion level was 20%. The accelerated corrosion time was calculated based on Faraday's first law as given below:

$$\text{Mass loss, } \quad m = \frac{t \cdot I \cdot M}{Z \cdot F} \qquad (1)$$

where m = mass loss, I = electrical current, t = applied time, F = Faraday's constant, M = molecular mass of steel and Z = valency number.

The specimens were soaked for 3 days prior to performing the accelerated corrosion. The corrosion test setup is shown in Fig. 2.

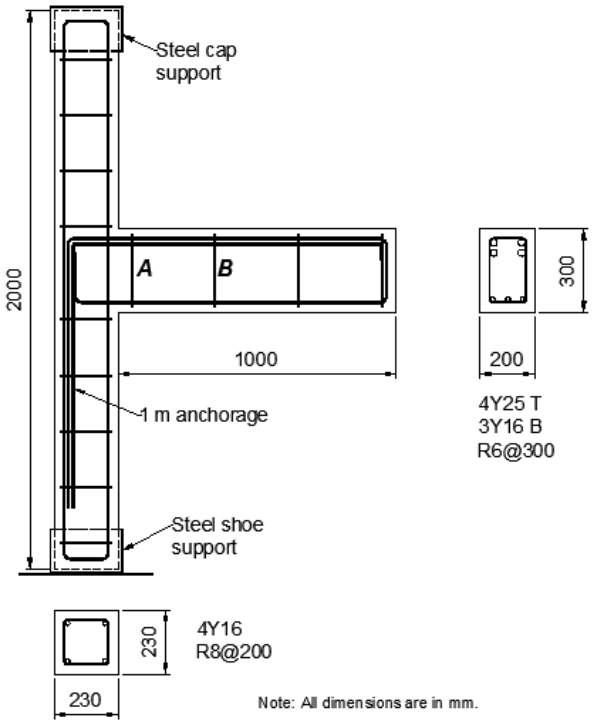

Figure 1. Beam to column dimensions and reinforcement detailing.

Figure 2. Corrosion process setup.

Only a targeted section of the shear links were corroded as indicated in Fig. 3. This section is 100 mm from each side of the closed shear link. Each side were corroded separately.

Corrosion was performed at two shear link positions '***A***' and '***B***' independently, as indicated in Fig. 1. Henceforth, specimens with corroded shear link at positions ***A*** and ***B***, will be denoted as specimen type *A* and type *B*, respectively. This provision will provide an indication on the shear load path near the joint region.

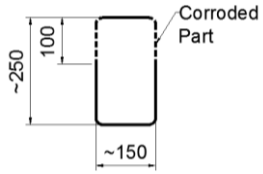

Figure 3. Corroded section of the shear link.

D. Test Setup and Procedure

The beam-to-column connection was setup as shown in Fig. 4. The top and bottom supports were encased in a purpose-built steel casing proving near pin supports. A hydraulic jack was used to apply the load at the end of the cantilever beam. The displacements were measured using six Linear Variable Displacement Transducers (LVDTs). LVDTs labelled 1 to 3 were used to record the vertical displacement whilst LVDTs A-C were used to record any lateral movements of the column. Constant loading rate of ~1mm/min was maintained throughout the test. The crack pattern was monitored and the respective load was labelled on the beam to understand the evolution of the cracks.

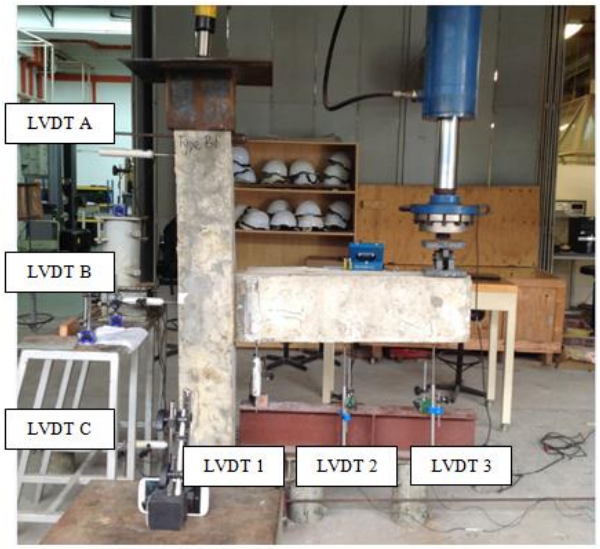

Figure 4. Experimental setup.

III. Results and Discussion

A. Concrete Compressive Strength

The compressive strengths of the concrete batches were within the targeted strength designed. Table I shows the 28 days compressive strength recorded for the two batches of concrete. The slump measured for the two batches were 120 mm and 130 mm for Type *A* and *B*, respectively.

B. Mass Loss

The actual mass loss was measured by extracting the corroded section of the shear link, cleaning and measuring the mass loss. The cleaning was performed using diluted hydrochloric acid to remove the corroded products. Detailed mass loss percentages are given in Table II. An example of the cleaned steel for sample *A1* is shown in Fig. 5. The losses are close to the targeted 20%.

TABLE I. 28 Days Concrete Compressive Strength

Sample No.	Compression Test Cubes (MPa)	
	Type *A*	**Type *B***
Sample 1	34.22	31.56
Sample 2	34.67	32.89
Sample 3	33.33	33.33
Average	34.07	32.59

TABLE II. Percentage Mass Loss for the Two Legs of All the Samples

Specimen	Shear Link No.	Mass Loss (%)
Type *A1*	*A1* (L)	22.92
	A1 (R)	22.69
Type *A2*	*A2* (L)	20.79
	A2 (R)	22.53
Type *A3*	*A3* (L)	24.68
	A3 (R)	20.81
Type *B1*	*B1* (L)	19.82
	B1 (R)	22.31
Type *B2*	*B2* (L)	21.39
	B2 (R)	22.13
Type *B3*	*B3* (L)	20.08
	B3 (R)	23.15

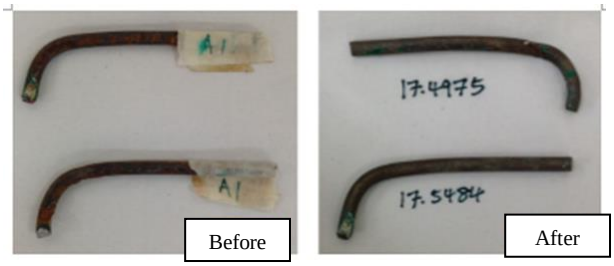

Figure 5. Type *A1* shear link section "before" and "after" cleaning.

C. Load-Displacement Behaviour

The load-displacement curve is a good indication of the failure behaviour of the structure. For clarity, the two types *A* and *B* samples are plotted separately. Fig. 6 shows the behaviour of samples type *A1* to *A3* compared to its control specimen. It should be noted that both control specimens are similar but casted separately. As it can be seen, the corroded specimens reached ultimate strengths of 63.8 kN, 61.1 kN and 62.4 kN for *A1*, *A2* and A3, respectively. In comparison with the control which reached 73.7 kN, the losses in absolute strength were 13.4%, 17.0% and 15.3% for *A1-A3*. There is no noticeable change in the ductility of the specimens.

A similar trend was observed for the samples type *B*. The load-displacement plot is shown in Fig. 7. The ultimate load for B1, B2 and B3 were 61.3 kN, 62.2 kN

and 62.5 kN, respectively. The control beam reached an ultimate load of 73.9 kN. This represents losses of 17.1%, 15.6% and 15.5% for *B1*, *B2* and *B3*, respectively. This set of specimens showed a clear reduction in ductility of the corroded specimens.

Fig. 8 shows a compilation of all the samples for LVDT position 3. It is can be seen that the two types *A* and *B* have similar reduction in strength but from this plot, it is hard to notice any reduction in rotational stiffness. Hence, the next section compares the moment-rotation plots for the tested specimens.

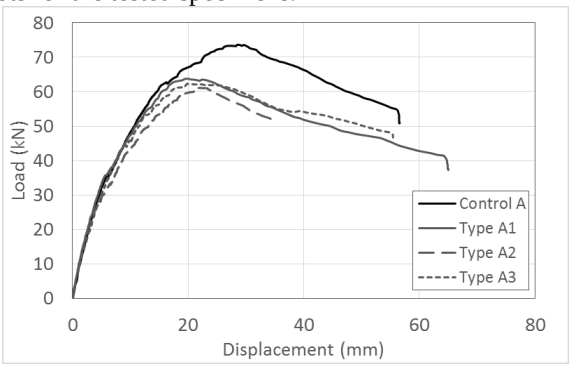

Figure 6. Load versus displacement at LVDT position 3 for Type *A* samples.

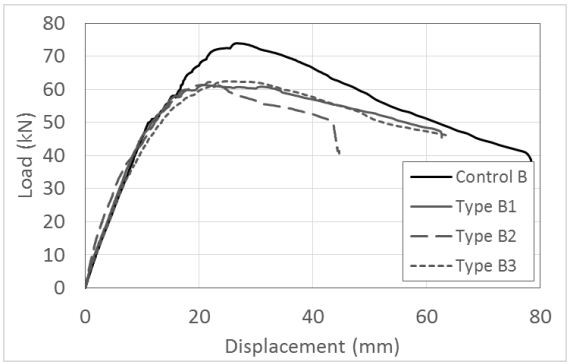

Figure 7. Load versus displacement at LVDT position 3 for Type *B* samples.

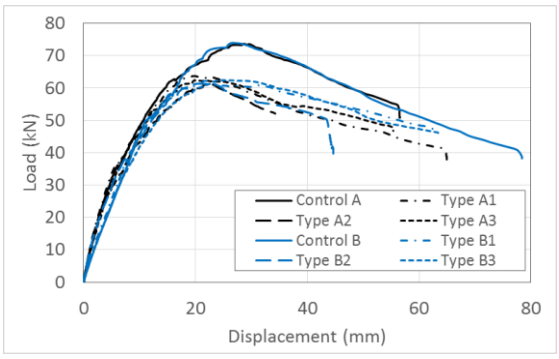

Figure 8. Load versus displacement at LVDT position 3 for both Type *A* and *B* samples.

D. Moment-Rotation Behaviour

The rotation of the beam was measured by calculating the relative displacement at LVDT 1 with respect to LVDT B to obtain the net rotation. The moment was calculated based on the lever arm from the loading point to the centre of the column. Fig. 9 shows the moment-rotation plot for all the samples. The full lines show the M-θ curves for the control specimens. There is a clear distinction in the initial rotational stiffness. In order to quantify the rotational stiffness, a pre-determined moment of approximately 30 kNm was selected as the reference to compute the rotational stiffness for all the specimens. The results are provided in Table III. In addition to having greater moment resistance, the control beams have higher rotational stiffness which shows that the reduction in shear capacity directly affect the joint stiffness.

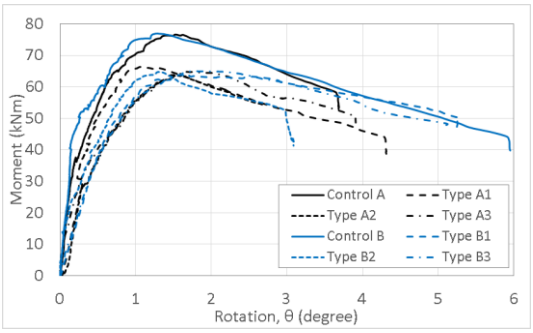

Figure 9. Moment-rotation plot for all the samples.

TABLE III. ROTATIONAL STIFFNESS CALCULATED AT 30 KNM

Sample No.	Rotational Stiffness (kNmrad^{-1})	
	Type *A*	**Type *B***
Control	11365	13845
1	7699	4443
2	4590	6031
3	6370	4549
Average (1-3)	6220	5008

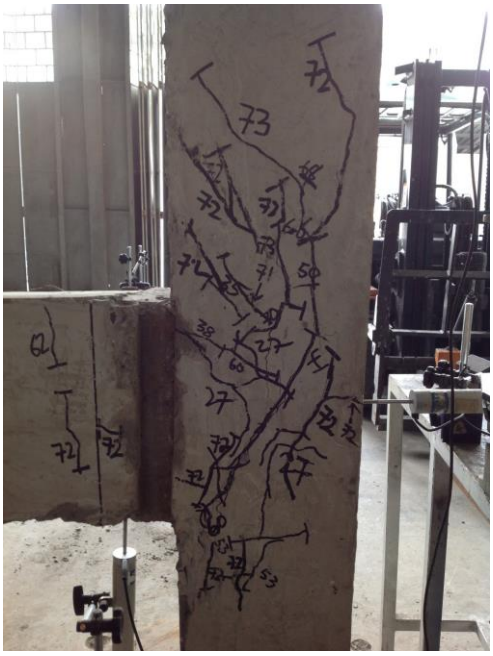

Figure 10. Crack formation at the joint for Sample – Control *A*.

Figure 11. Crack formation for sample *A1*.

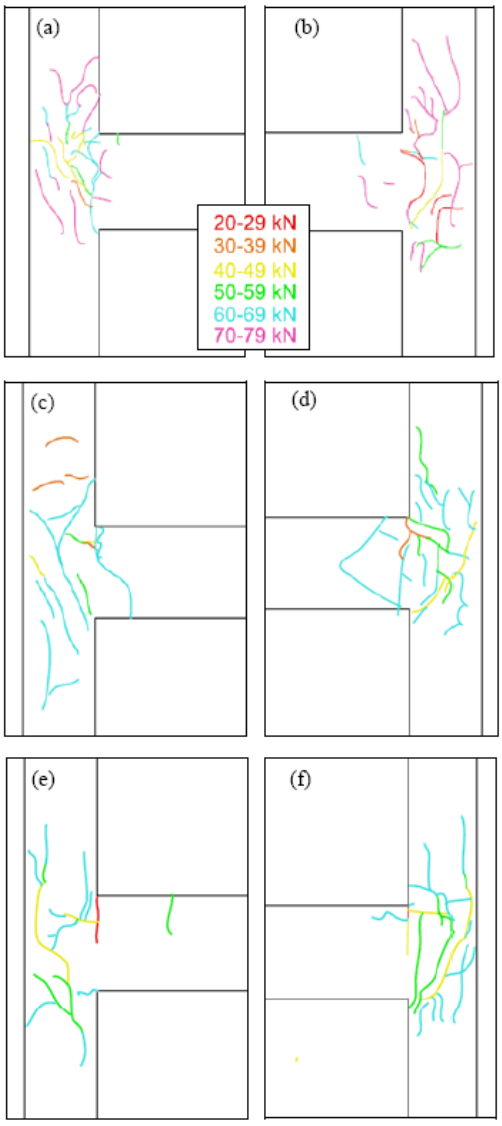

Figure 12. Crack pattern for the two sides of (a)-(b) control sample *A;* (c)-(d) sample *A1* and; (e)-(f) sample *B1*.

E. Cracking Pattern and Failure Mechanism

The failure mechanism was closely monitored throughout the test and the cracks formation was recorded. All the samples failed in a similar fashion, with the initial crack forming at the beam-to-column joint region. The crack patterns for sample *A* – control and *A1* are shown in Fig. 10 and Fig. 11, respectively for illustration. The sketches of the crack patterns for samples *A* (control), *A1* and *B1* are provided in Fig. 12.

It can be observed from Fig. 12 (a) and (b) that the cracks are mostly focused at the joint region without any cracks forming in the beam. In addition, some cracks are formed at higher loads compared to samples *A1* and *B1*. Fig. 12 (c) and (d) show some diagonal cracks in the beam region reflecting the lower resistance to shear due to the corroded shear link closer to the joint. It is interesting to note that there are also very little cracks formed in the beam for samples *B1* (Fig. 12e and f). There is one crack around the 50 kN range probably resulting from the yielding of the corroded shear yield in that region. It also confirmed that the load gets mobilised at the link closer to the applied load before reaching the joint.

IV. Conclusion

This study has detailed the structural performance deterioration of a beam-to-column connection as a result of shear link corrosion in the beam. It has interpreted the failure mechanism resulting from the corrosion by evaluating the crack patterns. The main findings are as follows:

(i) There was a significant reduction in the ultimate strength ranging from 13.5% to 17% due to the shear link corrosion.

(ii) The rotational stiffness was reduced from 11,365 $kNmrad^{-1}$ to an average of 6,220 $kNmrad^{-1}$ for samples Type *A* and, from 13,845 $kNmrad^{-1}$ to an average of 5,008 $kNmrad^{-1}$ for samples Type *B*.

(iii) Although the final failure occurred within the joint, there were signs of deterioration in the beam observed through the crack formation.

(iv) The crack pattern also showed the shear strength effect on the load path.

Acknowledgment

The author wishes to thank Tan Hann Chyuan who performed part of the experiments for his final year undergraduate project. This work was supported in part by a grant from Curtin Sarawak Research Fund.

References

[1] C. Fang, *et al*., "Corrosion influence on bond in reinforced concrete," *Cement and Concrete Research*, vol. 34, no. 11, pp. 2159-2167, 2004.

[2] H. S. Lee, T. Noguchi, and F. Tomosawa, "Evaluation of the bond properties between concrete and reinforcement as a function of the degree of reinforcement corrosion," *Cement and Concrete Research*, vol. 32, no. 8, pp. 1313-1318, 2002.

[3] R. Al-Hammoud, K. Soudki, and T. H. Topper, "Confinement effect on the bond behaviour of beams under static and repeated

loading," *Construction and Building Materials*, vol. 40, pp. 934-943, 2013.
[4] L. Chung, J. H. Jay Kim, and S. T. Yi, "Bond strength prediction for reinforced concrete members with highly corroded reinforcing bars," *Cement and Concrete Composites*, vol. 30, no. 7, pp. 603-611, 2008.
[5] X. H. Wang, *et al*., "Effect of bond and corrosion within partial length on shear behaviour and load capacity of RC beam," *Construction and Building Materials*, vol. 25, no. 4, pp. 1812-1823, 2011.
[6] C. Higgins and W. C. Farrow, "Tests of reinforced concrete beams with corrosion-damaged stirrups," *ACI Structural Journal*, vol. 103, no. 1, pp. 133-141, 2006.
[7] C. Suffern, A. El-Sayed, and K. Soudki, "Shear strength of disturbed regions with corroded stirrups in reinforced concrete beams," *Can. J. Civ. Eng.*, vol. 37, pp. 1045-1056, 2010.
[8] R. Azam and K. Soudki, "Structural performance of shear-critical RC deep beams with corroded longitudinal steel reinforcement," *Cement and Concrete Composites*, vol. 34, no. 8, pp. 946-957, 2012.
[9] R. Azam and K. Soudki, "Structural behavior of shear-critical rc slender beams with corroded properly anchored longitudinal steel reinforcement," *Journal of Structural Engineering*, vol. 139, no. 12, pp. 04013011, 2012.
[10] J. Rodriguez, L. M. Ortega, and J. Casal, "Load carrying capacity of concrete structures with corroded reinforcement," *Construction and Building Materials*, vol. 11, no. 4, pp. 239-248, 1997.
[11] J. Xia, W. L. Jin, and L. Y. Li, "Shear performance of reinforced concrete beams with corroded stirrups in chloride environment," *Corrosion Science*, vol. 53, no. 5, pp. 1794-1805, 2011.
[12] W. Zhu, *et al*., "Effect of corrosion of reinforcement on the mechanical behaviour of highly corroded RC beams," *Engineering Structures*, vol. 56, pp. 544-554, 2013.
[13] M. Lachemi, *et al*., "The effect of corrosion on shear behavior of reinforced self-consolidating concrete beams," *Engineering Structures*, vol. 79, pp. 1-12, 2014.
[14] K. Kobayashi, "Effect of bond and dowel action on shear capacity of RC beams," in *Proc. Tenth World Conference on Earthquake Engineering*, Madrid, Spain, 1992, pp. 3101-3106.
[15] M. N. Khaja and E. G. Sherwood, "Does the shear strength of reinforced concrete beams and slabs depend upon the flexural reinforcement ratio or the reinforcement strain?" *Canadian Journal of Civil Engineering*, vol. 40, no. 11, pp. 1068, 2013.
[16] M. Słowik, "Shear failure mechanism in concrete beams" *Procedia Materials Science*, vol. 3, pp. 1977-1982, 2014.
[17] S. Pantazopoulou and J. Bonacci, "Consideration of questions about beam-column joints," *ACI Structural Journal*, vol. 89, no. 1, pp. 27-36, 1992.
[18] G. M. S. Alva and A. L. H. C. El Debs, "Moment–rotation relationship of rc beam-column connections: Experimental tests and analytical model," *Engineering Structures*, vol. 56, pp. 1427-1438, 2013.
[19] Standards Australia, AS 3600-2009: Concrete Structures, 2009.

Charles K. S. Moy holds a BEng. (1st Class Hons) in Civil Engineering from the University of Mauritius, and a MEng. in Structural and Foundation Engineering and a PhD in Structural Engineering from the University of Sydney, Australia. His research interests include corrosion of reinforced concrete structures, steel-concrete composites, fibre reinforced polymer, textile reinforced mortar and multiscale material property investigation.

Currently, he is a Lecturer in Structural and Materials Engineering in the department of Civil Engineering at Xi'an Jiaotong-Liverpool University (XJTLU), Suzhou, China. Prior to joining XJTLU, he was a Senior Lecturer at Curtin University. He also worked in the consulting industry for a number of years, designing complex Civil and Structural Engineering facilities.

Dr. Moy is a Chartered Professional Engineer with Engineers Australia for the Civil and Structural Engineering colleges and is registered with the National Professional Engineers Register (Australia).